Multivariable L 1 Adaptive Depth and Attitude Control of MEROS Underwater Robot With Real-Time Experiments

Lotfi Chikh, Ahmed Chemori, Sifan Wang

Multivariable $\mathcal{L}_1$ Adaptive Depth and Attitude Control of MEROS Underwater Robot With Real-Time Experiments

L. Chikh * **A. Chemori** ** **S. Wang** ***

* *TECNALIA FRANCE, 950 rue Saint Priest, 34090 Montpellier, France, (e-mail: lotfi.chikh@tecnalia.com).*
** *LIRMM, University of Montpellier, CNRS, Montpellier, France, (e-mail: Ahmed.Chemori@lirmm.fr)*
*** *TECNALIA FRANCE, 950 rue Saint Priest, 34090 Montpellier, France, (e-mail: wangsifan4@gmail.com)*

Abstract: This paper deals with $\mathcal{L}_1$ adaptive control of a novel omnidirectional underwater vehicle called MEROS. To the best of our knowledge, this is the first study of depth and attitude (i.e. ϕ, θ, and ψ) tracking control on an underwater vehicle. We experimentally prove the effectiveness of the proposed control approach by commanding in closed-loop simultaneously the four aforementioned degrees of freedom (DoFs). The dynamic model of MEROS is highly nonlinear with coupling effects between the different DoFs making its stabilization and tracking control more challenging than conventional ROVs (remotely operated vehicles). Therefore, the use of a robust controller becomes essential, and the proposed scheme allows to ensure robustness whilst fast adaptation is achieved. Real-time experiments are performed to show the effectiveness of the proposed control design.

Keywords: Underwater robot, Mechatronic systems, Motion Control, Autonomous robotic systems, Attitude control, Robotics technology, $\mathcal{L}_1$ adaptive control.

1. INTRODUCTION

During the last decades, small and medium ROVs, able to perform complex inspection tasks are getting an increasing attention in many applications including ship hull inspection, scientific and archaeological researches, aquaculture farms, dams and wind parks inspection, and also military applications. For those tasks, the need of a sophisticated control solution in order to successfully perform the aforementioned mission is of high interest. Typically, the robot should be able to follow a desired reference trajectory autonomously in spite of external disturbances and parametric uncertainties.

Different advanced control techniques have been proposed so far in the literature in order to perform this objective. One can cite nonlinear PID control Guerrero et al. (2020b), model predictive control Molero et al. (2011), robust $\mathcal{H}_\infty$ control Roche et al. (2011), sliding mode control Pisano and Usai (2004); Shehu Tijjani et al. (2021), intelligent control Chang and Liu (2003), adaptive control Maalouf et al. (2015a), inverse dynamics control Salumae et al. (2016), and data-fusion control Remmas et al. (2021). These studies highlighted two important points related to underwater vehicles control. First, their dynamic models are difficult to identify because of their inherent nonlinearities and their evolution in a changing environment (salinity, buoyancy, currents,etc.). The second point is related to the robustness which is an important issue (persistent presence of external disturbances, unknown parameters, unprecise estimation). This motivates the development of adaptive controllers for such systems by many authors Guerrero et al. (2020a); Shehu Tijjani et al. (2021); Sun and Cheah (2009); Zhao and Yuh (2005). In these studies, the presented controllers have some drawbacks such as: a) the necessity of an adequate parameter initialization depending on the system configuration, we loose then the intuitiveness in the control tunning b) the increase in the adaptation gains that may lead to instability Antonelli (2007) and therefore, a compromise with good performances has to be found, and c) The need for the persistency in excitation can lead to a bad transient behaviour. To avoid the aforementioned drawbacks in adaptive control, Hovakimyan and Cao (2010) proposed $\mathcal{L}_1$ adaptive control in order to guarantee robustness performances decoupled from adaptation. Indeed, it has the major advantage of ensuring good performances without any need of appropriate parameter initialization as it was shown on a small ROV in Maalouf et al. (2012, 2015b) for only 2 DoFs.

In most of the mentioned studies, the authors presented either only simulation results Fjelstad and Fossen (1994); Li et al. (2004); Perrier and Canudas-De-Wit (1996); Roche et al. (2011); Sun and Cheah (2009) or real-time experiments on one DoF close-loop control Smallwood and Whitcomb (2002) Molero et al. (2011) or two DoFs Kreuzer (1996); Steenson et al. (2012). Some authors presented a simultaneous control of position (x, y and z) Yuh and Nie (2000), and others presented position and yaw control Hoang and Kreuzer (2008), or in some cases a stabilization of pitch and roll is added without any change in the desired attitude Zhao and Yuh (2005). According to our best knowledge, this is the first study presenting trajectory tracking of attitude (yaw pitch roll) which is necessary for complex inspection tasks.

The depth (z) is also controlled in closed-loop and the two remaining translational degrees of freedom (x and y for surge

and sway) are controlled in open loop by an operator. We talk about co-control concept: the goal here is to design a ROV with advanced capabilities (especially in orientations) while facilitating the inspection tasks enabling its control by one operator with no experience [1] . The choice of not instrumenting the surge and sway is motivated by our desire to design a compact and relatively inexpensive ROV for a larger industrial use.

The rest of the paper is organized as follows. In section 2, MEROS prototype is presented as well as its dynamic modeling. In section 3, the proposed $\mathcal{L}_1$ adaptive control theory and its application to MEROS model are introduced. Then, the obtained experimental results are presented and discussed in section 4. Finally, conclusions and future works are given in the last section.

2. DESCRIPTION AND MODELLING OF MEROS UNDERWATER VEHICLE

2.1 Description of the underwater vehicle MEROS

MEROS is a six-degree-of-freedom omnidirectional underwater vehicle controlled by six thrusters Izard et al. (2015). It is shown in figure 1. It has been designed for inspection tasks up to $100m$ of maximum depth. It is a mini-ROV that can be carried by one operator as it has a weight of only $13Kg$. Four degrees of freedom are controlled in closed loop (depth, roll, pitch, yaw), the two remaining degrees of freedom (translation X and Y) being controlled with a gamepad in open loop by the operator.

Fig. 1. General view of MEROS underwater vehicle.

MEROS was inspired from Pierrot et al. (1998) but adapted after some simulations (using Solidworks Flow Simulation) in order to limit the hydrodynamic effects between the thrusters. Two sensors are used: a pressure sensor (Series 33X from Keller) for depth and an inertial measurement unit (MTi from Xsens) for getting the orientation and the angular velocities. The IMU is the only sensor that may give data (acceleration) of surge and sway, but it is not enough accurate (drift effect due to integration) to be used for feedback control. MEROS has an isotropic configuration: the same forces and torques are possible in six DoFs. This may add some challenging issues in the control design due to the coupling effects and possible hydrodynamic disturbing forces. The necessity of designing a compact and low cost vehicle was also taken into account in the thruster choice. Indeed, the most suitable propellers in terms of compactness, cost and performance, were the model 280 from Tecnadyne. They have the major advantage of being compact enough when embedding an integrated controller which facilitates greatly the electronic design of the ROV. The control is performed through a computer and communication is done via the $90\,m$ umbilical that embed a power cable for the thrusters and an RS485 cable for communicating with the sensors.

[1] Currently, industrial ROVs need at least two operators, one experienced operator for controlling the ROV, and a second one for visual inspection.

2.2 MEROS kinematics and dynamics

Kinematic model The kinematics of an underwater vehicle can be expressed in two frames (figure 2): the earth-fixed frame (x_e, y_e, z_e) and the body-fixed frame (x_b, y_b, z_b). They are represented by the following vectors:

$$\eta = [x, y, z, \phi, \theta, \psi] \tag{1}$$

$$v = [u, v, w, p, q, r] \tag{2}$$

$$\dot{\eta} = J(\eta)v \tag{3}$$

η is the vector of cartesian positions and Euler angles in the earth-fixed frame space, v is the vector of velocities in the body-fixed frame and $J(\eta) \in \mathbb{R}^{6\times6}$ represents the jacobian transformation matrix mapping the body and earth-fixed frames.

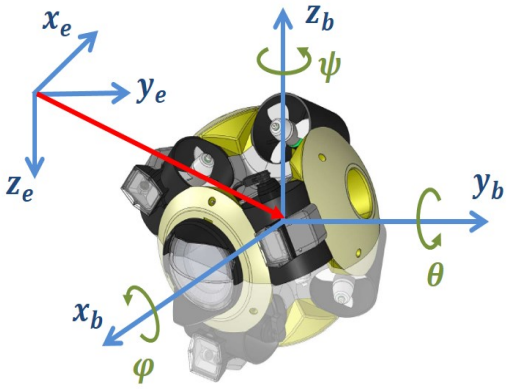

Fig. 2. Illustration of the reference frames of MEROS (x_e, y_e, z_e: earth-fixed frame,x_b, y_b, z_b: body-fixed frame).

Dynamic model The dynamic model of a ROV makes the link between the forces/torques applied on the vehicle and its positions, velocities and accelerations. A general model was proposed by Fossen (2002), and is based on SNAME notations. It can be written in a matrix form as:

$$M\dot{v} + C(v)v + D(v)v + g(\eta) = \tau + \omega_d \tag{4}$$

where the model matrices $M \in \mathbb{R}^{6\times6}$, $C \in \mathbb{R}^{6\times6}$ and $D \in \mathbb{R}^{6\times6}$ represent respectively the inertia (including added mass), Coriolis-Centripetal forces, and damping. g is the vector of weight and buoyancy. $\tau \in \mathbb{R}^{6\times1}$ represents the vector of the control inputs and $\omega_d \in \mathbb{R}^{6\times1}$ represents external disturbances. As in Maalouf et al. (2015b), and as the final use of the robot will be for inspection tasks a relatively low velocity, we assume that Coriolis terms can be neglected $C(v)v \approx 0$ leading to:

$$M\dot{v} + D(v)v + g(\eta) = \tau + \omega_d \tag{5}$$

Equation (5) expresses the dynamics in the body-fixed frame, and it can be transformed in the earth-fixed frame using the following transformations Fossen (2002) :

$$
\begin{aligned}
&\dot{\eta} = J(\eta)v \\
&\ddot{\eta} = J(\eta)\dot{v} + \dot{J}(\eta)v \\
&M^*(\eta) = J^{-T}(\eta)MJ^{-1}(\eta) \\
&D^*(v,\eta) = J^{-T}(\eta)D(v)J^{-1}(\eta) \\
&g^*(\eta) = J^{-T}(\eta)g(\eta) \\
&\tau^* = J^{-T}(\eta)\tau \\
&\omega_d^* = J^{-T}(\eta)\omega_d
\end{aligned}
\tag{6}
$$

with $J^{-T} = \left(J^{-1}\right)^T$. The vehicle's dynamics in the earth-fixed frame can be expressed as follows:

$$
M^*(\eta)\ddot{\eta} + D^*(v,\eta)\dot{\eta} + g^*(\eta) = \tau^* + \omega_d^* \tag{7}
$$

The general model (7) describes the dynamics of the vehicle in its full six DoFs. In our case, as only four DoFs are studied and controlled in close loop, it is possible to extract from (7) the equations of interest in order to obtain a reduced model in the earth-fixed frame:

$$
\begin{bmatrix} M_z^* & 0 & 0 & 0 \\ 0 & M_\varphi^* & 0 & 0 \\ 0 & 0 & M_\theta^* & 0 \\ 0 & 0 & 0 & M_\psi^* \end{bmatrix} \begin{bmatrix} \ddot{z} \\ \ddot{\varphi} \\ \ddot{\theta} \\ \ddot{\psi} \end{bmatrix} + \begin{bmatrix} D_z^* & 0 & 0 & 0 \\ 0 & D_\varphi^* & 0 & 0 \\ 0 & 0 & D_\theta^* & 0 \\ 0 & 0 & 0 & D_\psi^* \end{bmatrix} \begin{bmatrix} \dot{z} \\ \dot{\varphi} \\ \dot{\theta} \\ \dot{\psi} \end{bmatrix} + \begin{bmatrix} g_z^* \\ g_\varphi^* \\ g_\theta^* \\ g_\psi^* \end{bmatrix} = \begin{bmatrix} \tau_z^* + \omega_{d_z}^* \\ \tau_\varphi^* + \omega_{d_\varphi}^* \\ \tau_\theta^* + \omega_{d_\theta}^* \\ \tau_\psi^* + \omega_{d_\psi}^* \end{bmatrix} \tag{8}
$$

M_z^*, M_φ^*, M_θ^* and M_ψ^* are the mass parameters in the earth-fixed frame related to the degrees of freedom depth (Z), roll (φ), pitch (θ) and yaw (ψ). D_z^*, D_φ^*, D_θ^* and D_ψ^* are the damping parameters in the earth-fixed frame for these four degrees of freedom as well. The matrices of mass and damping are considered diagonal because of the spherical shape of the vehicle (cf. figure 1 and 2). The terms $g_i^*, \tau_i^*, \omega_{d_i}^*$ for $i = z, \varphi, \theta$ and ψ, represent respectively the weight/buoyancy components, the vector of control inputs and the external disturbances in the earth-fixed frame.

3. PROPOSED $\mathcal{L}_1$ ADAPTIVE CONTROL SOLUTION

3.1 Background on $\mathcal{L}_1$ Adaptive control

The $\mathcal{L}_1$ Adaptive control has been proposed by Hovakimyan and Cao (2010) and was applied to the control of a two degrees of freedom ROV in Maalouf et al. (2013, 2015b). In this paper, and as mentioned before we propose a more challenging problem which is the depth and attitude control of MEROS underwater vehicle presented in section 2. This controller can guarantee the fast convergence and the robustness at the same time. Its control architecture is illustrated in the block-diagram of Fig. 3. It includes four parts: the controlled system, the state predictor, the adaptation phase and the control law with a low pass filter. The role of the low pass filter is to cancel out the high frequencies that might occur in the control input which ensures a fast adaptation without altering the robustness. The details of each block in Fig. 3 are presented in the sequel:

- **Controlled system:**

Let us consider a class of nonlinear systems in which our system belongs to:

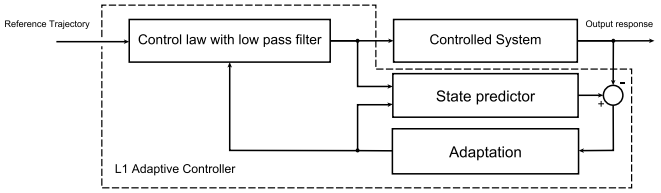

Fig. 3. Block diagram of the architecture based on the $\mathcal{L}_1$ adaptive controller Hovakimyan and Cao (2010).

$$
\begin{aligned}
&\dot{x}_1(t) = x_2(t), && x_1(0) = x_{10} \\
&\dot{x}_2(t) = f_2(t, x(t)) + \omega B_2 u(t), && x_2(0) = x_{20} \\
&y(t) = Cx(t)
\end{aligned}
\tag{9}
$$

$x_1(t) \in \mathbb{R}^n$ and $x_2(t) \in \mathbb{R}^n$ are the states of the system that constitute the state vector, that is: $x(t) = \left[x_1^T(t), x_2^T(t)\right]^T$. $u(t) \in \mathbb{R}^m$ is the vector of control inputs ($m \leq n$) and $\omega \in \mathbb{R}^{m\times m}$ represents an uncertainty on the control input. $B_2 \in \mathbb{R}^{n\times m}$ is a known constant matrix. $C \in \mathbb{R}^{m\times 2n}$ is a known full rank constant matrix. $y \in \mathbb{R}^m$ is the measured output. $f_2(t, x(t))$ is an unknown nonlinear function that represents the nonlinear dynamics of the system. This function is assumed to be bounded. According to Hovakimyan and Cao (2010), the function $f_2(t, x(t))$ can be written as $f_2(t, x(t)) = A_2 x_2 + \theta(t)\left\|x(t)\right\|_{\mathcal{L}_\infty} + \sigma(t)$. $A_2 \in \mathbb{R}^{n\times n}$is the state matrix representing the linear dynamic part of x_2. $\theta(t) \in \mathbb{R}^n$ and $\sigma(t) \in \mathbb{R}^n$ are the vectors of unknown time-varying parameters. $\left\|x(t)\right\|_{\mathcal{L}_\infty}$ is the infinity norm of the measured state. So the system of equations (9) can be rewritten as:

$$
\begin{aligned}
&\dot{x}(t) = \begin{bmatrix} 0_{n\times n} & \mathbb{I}_n \\ 0_{n\times n} & A_2 \end{bmatrix} \begin{bmatrix} x_1 \\ x_2 \end{bmatrix} + \begin{bmatrix} 0_{n\times 1} \\ \theta \end{bmatrix} \left\|x\right\|_{\mathcal{L}_\infty} + \begin{bmatrix} 0_{n\times 1} \\ \sigma \end{bmatrix} \omega u(t) \\
&y(t) = Cx(t)
\end{aligned}
\tag{10}
$$

Assuming that $A = \begin{bmatrix} 0_{n\times n} & \mathbb{I}_n \\ 0_{n\times n} & A_2 \end{bmatrix}$ is the state matrix representing the dynamics of the open-loop system. It can be modified into a Hurwitz matrix A_m of the desired dynamics of the closed-loop system with a static feedback gain $k_m \in \mathbb{R}^{m\times 2n}$. Let $A_m = A - B_m k_m$, with $B_m = \begin{bmatrix} 0_{n\times m} \\ B_2 \end{bmatrix}$. Finally, the system can be rewritten as follows:

$$
\begin{aligned}
&\dot{x}(t) = A_m x(t) + B_m(\omega u_a + \theta(t)\left\|x(t)\right\|_{\mathcal{L}_\infty} + \sigma(t)) \\
&x(0) = x_0 \\
&y(t) = Cx(t)
\end{aligned}
\tag{11}
$$

The control input is composed of two parts: $u = u_m + u_a$. $u_m = -k_m x$, k_m is used to transform matrix A into a Hurwitz matrix A_m. u_a is the control input used for the adaptation phase in the block-diagram of Fig. 3.

- **State predictor:**

The form of the state predictor is the same as the controlled system but using the estimated parameters obtained in the adaptation phase. It can be written as follows:

$$
\dot{\widehat{x}}(t) = A_m \widehat{x}(t) + B_m(\widehat{\omega} u_a + \widehat{\theta}(t)\left\|x(t)\right\|_{\mathcal{L}_\infty} + \widehat{\sigma}(t)) \tag{12}
$$

- **Adaptation:**

Our underwater vehicle is composed of three unknown parameters $\omega(t)$, $\theta(t)$ and $\sigma(t)$ with the estimated corresponding parameters: $\widehat{\omega}(t)$,$\widehat{\theta}(t)$ and $\widehat{\sigma}(t)$.

These parameters are estimated using the error between the controlled system and the state predictor, and a projection operator is used to ensure their boundedness. The adaptation law of each estimated parameter is written as follows:

$$\begin{aligned}\dot{\widehat{\theta}}(t) &= \Gamma proj(\widehat{\theta}(t), -(\widetilde{x}^T(t)PB_m)^T \left\|x(t)\right\|_{\mathcal{L}_\infty})\\ \dot{\widehat{\sigma}}(t) &= \Gamma proj(\widehat{\sigma}(t), -(\widetilde{x}^T(t)PB_m)^T)\\ \dot{\widehat{\omega}}(t) &= \Gamma proj(\widehat{\omega}(t), -(\widetilde{x}^T(t)PB_m)^T u_a^T(t))\end{aligned} \tag{13}$$

Γ is the adaptation gain and $\widetilde{x}(t) = \widehat{x}(t) - x(t)$ is the prediction error. P is the solution of the algebraic Lyapunov equation: $A_m^T P + PA_m^T = -Q$ for any arbitrary symmetric positive definite matrix $Q = Q^T > 0$.

- **Control law with low pass filter:**

The control input u_a is calculated with a low pass filter. It takes the following form in the Laplace domain:

$$u_a(s) = -kD(d)(\widehat{\eta}_l(s) - k_g r) \tag{14}$$

$$\widehat{\eta}_l = \widehat{\omega} u_a + \widehat{\theta}(t) \left\|x(t)\right\|_{\mathcal{L}_\infty} + \widehat{\sigma}(t) \tag{15}$$

k is a positive feedback gain, $D(s)$ is an $m \times m$ strictly proper transfer matrix that leads to the stable closed-loop filter: $C(s) = \frac{\omega k D(s)}{\mathbb{I}_m + \omega k D(s)}$ where s is the Laplace variable. $k_g = -(CA_m^{-1}B_m)^{-1}$ is a feed-forward pre-filter applied to the reference signal $r(t)$. The feedback gain k and the filter $D(s)$ must be chosen to fulfill the $\mathcal{L}_1$ norm condition in order to ensure the stability of the closed-loop system. The proof of stability can be found in Hovakimyan and Cao (2010).

The overall control architecture is detailed in the block-diagram of Fig. 4.

3.2 Application to control MEROS underwater vehicle

In this paper, the architecture $\mathcal{L}_1$ adaptive control architecture is applied to control four degrees of freedom (depth and attitude of MEROS vehicle). Combining equations (8) and (10) gives:

$$\begin{bmatrix}\dot{\eta}_1\\ \dot{\eta}_2\end{bmatrix} = \begin{bmatrix}0_{4\times4} & \mathbb{I}_4\\ 0_{4\times4} & \frac{-D_r^*}{M_r^*}\end{bmatrix}\begin{bmatrix}\eta_1\\ \eta_2\end{bmatrix} - \begin{bmatrix}0_{4\times4}\\ \frac{-g_r^*}{M_r^*} - \frac{-\omega_r^*}{M_r^*}\end{bmatrix} + \begin{bmatrix}0_{4\times4}\\ \frac{1}{M_r^*}\end{bmatrix}\omega\tau_*^r \tag{16}$$

In this equation, $\eta_1 = \left[z\ \varphi\ \theta\ \psi\right]^T$, $\eta_2 = \left[\dot{z}\ \dot{\varphi}\ \dot{\theta}\ \dot{\psi}\right]^T$, and we consider $\omega \in \mathbb{R}^{4\times4}$ being an identity matrix (we assume that we have a good knowledge of the characteristics of the vehicle thrusters). D_r^* is a diagonal matrix with the following form:

$$D_r^* = diag\left\{D_z^*, D_\varphi^*, D_\theta^*, D_\psi^*\right\} \tag{17}$$

The same with M_r^*, g_r^* and ω_r^*. If we write equation (16) into the form of equation (11) with the state matrix A_m, we can obtain:

$$\begin{aligned}\begin{bmatrix}\dot{\eta}_1\\ \dot{\eta}_2\end{bmatrix} &= A_m\begin{bmatrix}\eta_1\\ \eta_2\end{bmatrix} + \begin{bmatrix}0_{4\times4}\\ \frac{1}{M_r^*}\end{bmatrix}\left(\omega u_a + \theta(t)\left\|\eta(t)\right\|_{\mathcal{L}_\infty} + \sigma(t)\right)\\ y &= \begin{bmatrix}1&0&0&0&0&0&0&0\\ 0&1&0&0&0&0&0&0\\ 0&0&1&0&0&0&0&0\\ 0&0&0&1&0&0&0&0\end{bmatrix}\begin{bmatrix}\eta_1\\ \eta_2\end{bmatrix} = \begin{bmatrix}z\\ \varphi\\ \theta\\ \psi\end{bmatrix}\end{aligned} \tag{18}$$

In this equation, $A_m \in \mathbb{R}^{8\times8}$ is a Hurwitz matrix obtained with k_m. $B_m = \begin{bmatrix}0_{4\times4}\\ \frac{1}{M_r^*}\end{bmatrix} \in \mathbb{R}^{8\times4}$. $\theta \in \mathbb{R}^4$ includes the uncertainties damping coefficients, with $\theta = \left[\Delta(-D_z^*), \Delta(-D_\varphi^*), \Delta(-D_\theta^*), \Delta(-D_\psi^*)\right]^T$ (Δ refers to the uncertainty). $\sigma \in \mathbb{R}^4$ includes the weight and buoyancy as well as the external disturbances, with $\sigma = \left[-g_z^* + \omega_{dz}^*, -g_\varphi^* + \omega_{d\varphi}^*, -g_\theta^* + \omega_{d\theta}^*, -g_\psi^* + \omega_{d\psi}^*\right]^T$. $\left\|\eta(t)\right\|_{\mathcal{L}_\infty}$ is the infinity norm of the state vector η at instant t. The control input $u = u_m + u_a$ is computed in the earth fixed frame. The system outputs are Z, φ, θ and ψ.

4. OBTAINED REAL-TIME EXPERIMENTAL RESULTS

In this section, the obtained experimental results are presented and discussed. The tests have been performed in a $5\,m^3$ pool without any input from the human user during the motions (i.e. autonomous mode). A large part of the umbilical is deployed in order to avoid any drag effect on the ROV. The reference tracking trajectory of each degree of freedom is described as follows: for Z, from $t = 0\,s$ to $t = 15\,s$, the depth decreases with $15\,cm$, at $t = 30$, the depth continues to fall $20\,cm$ and remains at this depth until $t = 210\,s$, then the depth decreases $20\,cm$. For φ, at $t = 70s$, the roll desired values rises by $30°$ and remains at this value until $t = 150\,s$, the desired roll returns to the initial value. For θ, at $t = 50\,s$, the pitch order steps up $15°$ and stays in this value until $t = 130\,s$, and then, it returns to its initial value. For ψ, at $t = 100\,s$, the desired yaw increases by $30°$ and stays in this value until $t = 170\,s$, the desired yaw returns to its initial value. The autonomously non-controlled DoFs (i.e. surge and sway) can be controlled in open loop by the human during shared control, where an interaction (due to the coupling in dynamics) is noticed. The values of the tuned parameters (through numerical simulations first, then finely adjusted during experiments) are summarized in Table 1.

Table 1. Summary of control design parameters.

Degree of freedom	Poles	Γ	k	$D(s)$	Initial values $\widehat{\theta}(0)$ and $\widehat{\sigma}(0)$
Z	$(-7,-3)$	10000	2	$\frac{1}{s}$	0
φ	$(-7,-4)$	45	1	$\frac{1}{s}$	0
θ	$(-7,-3)$	80	2	$\frac{1}{s}$	0
ψ	$(-7,-4)$	30	1.6	$\frac{1}{s}$	0

The results are presented in Fig. 5. We can observe in this scenario, that when four degrees of freedom are controlled, there are some oscillations that are more significant for the pitch and yaw angles. This can be due to the effect of the umbilical that introduces external torques due to its weight and the torsion brought by the high roll desired angle. We also observe that these oscillations are more significant when there is a change in the desired trajectory of another DoF and this is logically due to the isotropic design of MEROS and the coupling effect. In general, when the four DoFs are controlled simultaneously we expect more hydrodynamic effects (even if the design was optimized to limit them) and this may have an additional disturbing effect. In terms of control inputs, there are no saturation effects. We also suppose that the numerical derivative used in the estimation of the velocities can be replaced by an observer in order to avoid the possible amplification of the measurement noise.

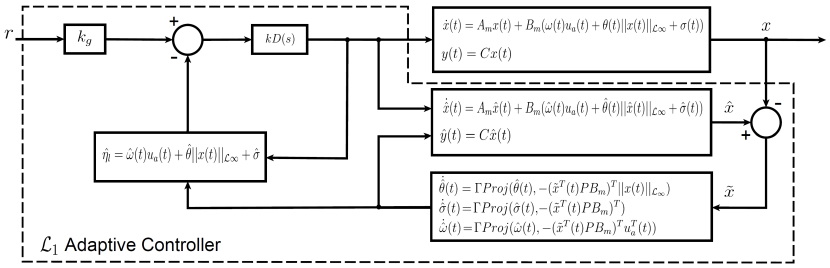

Fig. 4. Detailed block-diagram of the $\mathcal{L}_1$ adaptive controller architecture Hovakimyan and Cao (2010).

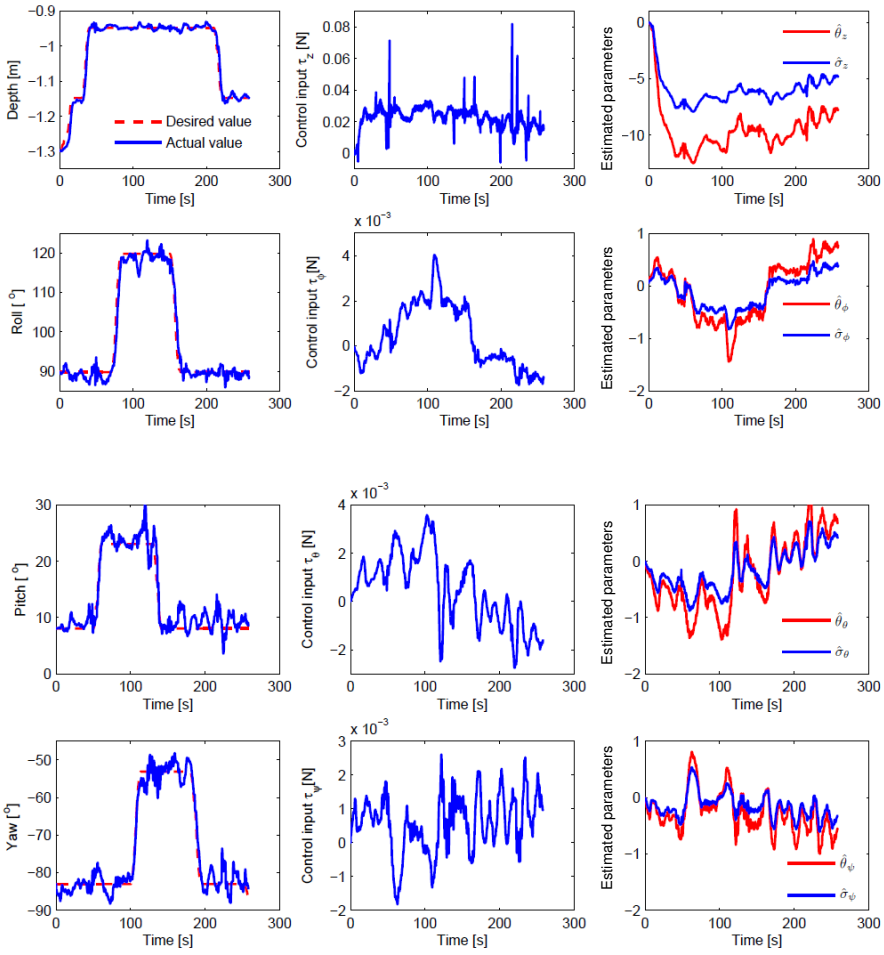

Fig. 5. Obtained real-time experimental results: Simultaneous control of depth, roll, pitch and yaw. (Left) evolution versus time of the controlled degrees of freedom w.r.t their respective reference trajectories, (Middle) evolution of their corresponding control inputs, (right) evolution versus time of the estimated parameters.

5. CONCLUSION AND FUTURE WORK

This paper deals with the control of an omnidirectional underwater vehicle. The proposed control solution, based on $\mathcal{L}_1$ adaptive control, has been experimentally validated for 4 DOFs (attitude and depth). Another interesting result is the ability of such a robust control to manage the strong couplings due to the isotropic design of the robot. These results have been obtained despite the relatively simplified model and this proves the effectiveness and robustness of the proposed $\mathcal{L}_1$ adaptive control. In the future, we would like to consider some enhancements through the use of the quaternion representation and take full advantage of the omnidirectional possibilities during inspection tasks. Furthermore, we observed that the umbilical of the robot is too stiff and may have a destabilizing effect on the vehicle (oscillations). Consequently, a new design of the umbilical can be planned. Besides, further tests and experiments will be performed in open water, with real operating conditions like dam or harbor inspection in order to confront the ROV to more realistic challenging applications.

REFERENCES

Antonelli, G. (2007). On the use of adaptive/integral actions for six-degrees-of-freedom control of autonomous underwater vehicles. *IEEE Journal of Oceanic Engineering*, 32, 300312.

Chang, M. Chang, W. and Liu, H. (2003). Model-based fuzzy modeling and control for autonomous underwater vehicles in the horizontal plane. *Journal of Marine Sciences and Technology*, 11, 155–163.

Fjelstad, O.E. and Fossen, T. (eds.) (1994). *Singularity-free tracking of unmanned underwater vehicles in 6 DOF*. Proceedings of the 33rd IEEE Conference on Decision and Control, IEEE, FL, USA, pp 1128-1133.

Fossen, T. (2002). *Marine Control Systems:Guidance, Navigation and Control of Ships, Rigs and Underwater Vehicles*.

Guerrero, J., Torres, J., Creuze, V., and Chemori, A. (2020a). Adaptive disturbance observer for the trajectory tracking of underwater vehicles. *Ocean Engineering*, 200, 107080.

Guerrero, J., Torres, J., Creuze, V., and Chemori, A. (2020b). Observation based nonlinear pd control for robust trajectory tracking for autonomous underwater vehicles. *IEEE Journal of Oceanic Engineering*, 45(4), 1190–1202.

Hoang, N. and Kreuzer, E. (2008). A robust adaptive sliding mode controller for remotely operated vehicles. *Tech. Mech.*, 3-4, 185–193.

Hovakimyan, N. and Cao, C. (2010). *L1 Adaptive Control Theory*. SIAM.

Izard, J.B., Chikh, L., Collado, V., and Auffray, V. (2015). An omnidirectional underwater robot. Patent: PCT/EP2015/081194.

Kreuzer, Edwin & C. Pinto, F. (1996). Controlling the position of a remotely operated underwater vehicle. *Applied Mathematics and Computation*.

Li, J.H., Lee, P.M., and Jun, B.H. (2004). An adaptive nonlinear controller for diving motion of an AUV. In *Oceans'04 MTS/IEEE Techno-Ocean '04 (IEEE Cat. No.04CH37600)*, volume 1, 282–287.

Maalouf, D., Chemori, A., and Creuze, V. (2013). Stability analysis of a new extended l1 controller with experimental validation on an underwater vehicle. In *IEEE CDC*. Florence, Italy.

Maalouf, D., Creuze, V., and Chemori, A. (2012). A novel application of multivariable l1 adaptive control: From design to real-time implementation on an underwater vehicle. In *IEEE/RSJ IROS*. Algarve, Portugal.

Maalouf, D., Creuze, V., Chemori, A., Campos, E., Torres Tamanja, I., Torres Munoz, J., Lozano, R., and Tempier, O. (2015a). Real-time experimental comparison of two depth control schemes for underwater vehicles. *International Journal of Advanced Robotics Systems*, 12(2), 1–15.

Maalouf, D., Chemori, A., and Creuze, V. (2015b). L1 adaptive depth and pitch control of an underwater vehicle with real-time experiments. *Ocean Engineering*, 98, 66 – 77.

Molero, A., Dunia, R., and Fernandez, G. (2011). Model predictive control of remotely operated underwater vehicles. In *2011 50th IEEE Conference on Decision and Control and European Control Conference (CDC-ECC)*. Orlando, FL, USA.

Perrier, M. and Canudas-De-Wit, C. (1996). Experimental comparison of pid vs. pid plus nonlinear controller for subsea robots. *Autonomous Robots*, 3, 195–212. doi: 10.1007/BF00141155.

Pierrot, F., Benoit, M., and Dauchez, P. (1998). Optimal thruster configuration for omni-directional underwater vehicles. samos: a pythagorean solution. In *IEEE Oceanic Engineering Society. OCEANS'98. Conference Proceedings (Cat. No.98CH36259)*, volume 2, 655–659 vol.2. doi: 10.1109/OCEANS.1998.724320.

Pisano, A. and Usai, E. (2004). Output-feedback control of an underwater vehicle prototype by higher-order sliding modes. *Automatica*, 40(9), 1525 – 1531. doi: https://doi.org/10.1016/j.automatica.2004.03.016.

Remmas, W., Chemori, A., and Kruusmaa, M. (2021). Diver tracking in open waters: A low-cost approach based on visual and acoustic sensor fusion. *Journal of Field Robotics*, 38(3), 494–508.

Roche, E., Sename, O., Simon, D., and Varrier, S. (2011). A hierarchical varying sampling $\mathcal{H}_\infty$ control of an auv. In *18th IFAC World Congress*. Milano, Italy.

Salumae, T., Chemori, A., and Kruusmaa, M. (2016). Motion control architecture of a 4-fin u-cat auv using dof prioritizations. In *IEEE/RSJ IROS*. Daejeon, Korea.

Shehu Tijjani, A., Chemori, A., and V. Creuze, v. (2021). Robust adaptive tracking control of underwater vehicles: Design, stability analysis and experiments. *IEEE/ASME Transactions on Mechatronics*, 26(2), 897–907.

Smallwood, D. and Whitcomb, L. (2002). The effect of model accuracy and thruster saturation on tracking performance of model based controllers for underwater robotic vehicles: experimental results. In *Proceedings of the IEEE International Conference on Robotics and Automation*, 1081–1087. Washington DC, USA.

Steenson, L.V., Phillips, A.B., Rogers, E., Furlong, M.E., and Turnock, S.R. (2012). Experimental verification of a depth controller using model predictive control with constraints onboard a thruster actuated auv. *IFAC Proceedings Volumes*, 45(5), 275 – 280.

Sun, Y.S. and Cheah, C.C. (2009). Adaptive control schemes for autonomous underwater vehicle. *Robotica*, 27, 119–129.

Yuh, J. and Nie, J. (2000). Application of non-regressor-based adaptive control to underwater robots: Experiment. *Computers & Electrical Engineering*, 26, 169–179. doi: 10.1016/S0045-7906(99)00039-7.

Zhao, S. and Yuh, J. (2005). Experimental study on advanced underwater robot control. *IEEE Transactions on Robotics*, 21(4), 695–703. doi:10.1109/TRO.2005.844682.